Highly efficient energy and mass transfer in bcc metals by supersonic 2-crowdions

I. A. Shepelev[1],* D. V. Bachurin[2],† E. A. Korznikova[3,4,5],‡ and S. V. Dmitriev[4,5§]

[1]*Institute of Physics, Saratov State University, Saratov, Russia*

[2]*Institute for Applied Materials – Applied Materials Physics, Karlsruhe Institute of Technology, Eggenstein-Leopoldshafen 76344, Germany*

[3]*Ufa State Aviation Technical University, 450008 Ufa, Russia*

[4]*Institute of Molecule and Crystal Physics, Ufa Federal Research Center, Russian Academy of Sciences, Ufa Russia and*

[5]*Ufa State Petroleum Technological University, Ufa, Russia*

(Dated: April 11, 2023)

Abstract

During irradiation, bombardment with energetic particles, or plasma treatment, structural transformations occur in materials, in which point defects play a very important role. Highly mobile crowdions contribute to the transfer of mass and energy in the crystal lattice. Static and slowly moving crowdions are well studied, in contrast to crowdions moving at a speed exceeding the speed of sound. Here, for the first time, dynamics of supersonic N-crowdions ($N = 1, 2$) is investigated in bcc metals (tungsten and vanadium) with the help of molecular dynamics simulations. N-crowdions are excited by imparting sufficiently high initial velocities to N neighboring atoms located in the same close-packed atomic row along this row. Both supersonic 1- and 2-crowdions carry one interstitial atom each. Modeling shows that much less energy is required to excite a 2-crowdion compared to a 1-crowdion. Energy dissipation for a 2-crowdion is much slower than for a 1-crowdion suggesting that the supersonic 2-crowdion is an efficient mass transfer mechanism in bcc metals. The distance traveled by the supersonic 1- and 2-crowdions in W is much greater than in V. The supersonic crowdion in W transforms into a moving subsonic crowdion, and in V it transforms into a standing subsonic crowdion carrying a localized high-amplitude oscillation mode. These differences can be explained by the features of interatomic interactions in W and V.

Keywords: lattice defects, subsonic crowdion, supersonic crowdion, mass transfer, molecular dynamics simulations

I. INTRODUCTION

Extreme influences, such as laser treatment[1], severe plastic deformation[2], ultrafast loading[3,4], irradiation[5–10], plasma treatment[11], etc., cause irreversible changes in the crystal structure and lead to the transition of the lattice to a non-equilibrium state. In these processes, the atoms strongly deviate from their equilibrium lattice sites, and the nonlinear nature of the interatomic bonds begins to play a significant role. Such extreme impacts cause the appearance of an abnormally high concentration of point defects, called Frenkel pairs (vacancy and interstitial).

An interstitial atom can exist in many configurations, including the crowdion configuration, when it is located in a close-packed atomic row[12–14]. The migration ability of crowdions is much greater as compared to vacancies[2,15,16], which makes them efficient in mass transfer in materials. The high migration ability of crowdions leads to their rapid annihilation, hindering experimental analysis of their structure and movement[17]. Therefore, computer simulation methods are widely used, including methods of molecular dynamics[18–24], Monte Carlo[25,26], first-principles[27,28] and multiscale modelling[13,29–31].

If an atom in a close-packed row receives a large enough momentum along the row, it can replace a neighboring atom and initiate a replacement collision sequence (RCS) produced by a moving crowdion[32]. In this case, a Frenkel pair is formed, and the moving interstitial atom transfers mass. If the initial energy is below the threshold displacement energy, then a focuson sequence (FS) is realized[32]. After the focuson relaxation, the ideal crystal structure is restored.

Most of the studies analyze static or slowly moving crowdions and the elastic stress fields produced by them[27,31,33,34]. However, the interstitials produced under the above-mentioned extreme influences can propagate along close-packed atomic rows with the speed exceeding the speed of longitudinal sound. The supersonic motion of crowdions was studied in the two-dimensional triangular lattices[35–37], fcc lattices[28,38,39] and intermetallic compound Ni_3Al[40]. For bcc metals, as far as we know, the supersonic motion of crowdions has not yet been studied.

Metals with bcc lattice, such as tungsten and vanadium, are of particular interest due to the fact that they are planned to be widely used in the International Thermonuclear Experimental Reactor (ITER)[41]. Tungsten is considered as divertor material[42,43] and vanadium

alloys are promising materials for the first-wall and breeding blanket due to their outstanding thermal properties[44,45]. This is the reason for active studies on the defects in W[7–10,18,46–50] and V[44,51–54]. In order to demonstrate the difference between 1- and 2-crowdions, we provide two Supplemental files named 1_crowdion.gif and 2_crowdion.gif. Atoms are colored according to their kinetic energy. It can be seen that in the 2-crowdion two atoms move simultaneously at a high speed, while in the 1-crowdion one atom has a high speed. It is well-known that atomic collisions are focusing only if the collision velocity is below a critical value. The 2-crowdion with the fastest focusing speed carries twice as much energy as the 1-crowdion and therefore travels a longer distance.

Along with the supersonic 1-crowdions, the mass transfer by the supersonic N-crowdions, which were excited by giving an initial velocity to N neighboring atoms along the chosen close-packed atomic row, has been studied[35,38,39]. It turned out that supersonic N-crowdions can be excited with a lower energy and travel much longer distances than supersonic 1-crowdions. This is related to the fact that motion of supersonic N-crowdions for $N > 1$ is more self-focusing than that for $N = 1$[38,55].

Atomic collisions in a close-packed row with a velocity above a threshold level are defocusing, i.e., any small deviation of the velocity vector from the direction of the row will increase exponentially from atom to atom[38,55]. Collisions with speeds below the threshold are self-focusing, and the direction of the velocity vector in successive collisions will exponentially approach the direction of the atomic row. It follows from this that there is an upper limit on the energy that can be imparted to an atom to excite a supersonic 1-crowdion. This energy can be increased without increasing the speed of atoms, if not one, but N neighboring atoms are excited, creating a supersonic N-crowdion. Having more energy, an N-crowdion with $N > 1$ propagates to a longer distance than a 1-crowdion.

Simultaneous excitation of two atoms in an atomic row can be easily achieved by bombardment of crystal surface by biatomic molecules[39]. This fact is important for such applications as deposition, sputtering and ion implantation. We do not know whether supersonic 2-crowdions are formed in the collision cascades in metals under irradiation. Both supersonic 1- and 2-crowdions carry single interstitial and when they transform to subsonic crowdions they become indistinguishable.

The present work is aimed to study the energy and mass transfer in bcc metals (tungsten and vanadium) via supersonic N-crowdions by means of molecular dynamics simulations.

The emphasis is mainly on the physics of the observed process. The temperature effect is analyzed, while the influence of various imperfections (impurity atoms, point or extended defects, strain fields, etc.) is not considered here.

II. METHODOLOGY

The molecular dynamics method is ideally suited for the analysis of mass transfer by supersonic crowdions, taking into account the small spatial and temporal scales of the phenomenon under study. This method has established itself as a powerful tool in modern materials science with numerous applications to materials under extreme conditions, including the analysis of defect dynamics in various crystal lattices, both model and real[51,56–62], nonlinear dynamics of the crystal lattice[63–65], and exposure to radiation[57,66].

The molecular dynamics method is based on phenomenological interatomic potentials, which should be chosen taking into account the specific problem being solved. In materials under high-energy impacts, atoms collide with high velocities, and at short interatomic distances the repulsive part of the potentials becomes important. For this purpose, many-body interatomic potentials have been developed that describe well the behavior of metals under extreme conditions. In particular, the embedded atom method potentials have been adapted for bcc tungsten[67] and vanadium[52], which are widely used in fusion and fission reactors. Both the potentials are of Finnis-Sinclair type and are fitted to both the experimental and first principles calculation data. The total energy E_i of the i-th atom is given by:

$$E_i = F_\alpha \left(\sum_{j \neq i} \ \rho_{\alpha\beta}(r_{ij}) \right) + \tfrac{1}{2} \sum_{j \neq i} \phi_{\alpha\beta}(r_{ij}), \tag{1}$$

where $\rho_{\alpha\beta}$ refers to the electron density contributed by a neighboring j-th atom of element β at the site of i-th atom of element α. ρ is a functional specific to the elements of both i-th and j-th atoms, so that different elements can contribute differently to the total electron density at an atomic site depending on the element at this atomic site. These potentials are incorporated into the Large-scale Atomic/Molecular Massively Parallel Simulator (LAMMPS), which is used for molecular dynamics simulations.

The Cartesian coordinate axes are chosen so that the x axis is oriented along the $\langle 111 \rangle$ close-packed crystallographic direction. The translational cell has the shape of a parallelepiped and contains 8 atoms. The equilibrium bcc lattice parameters are $a_0 = 3.14$ Å for

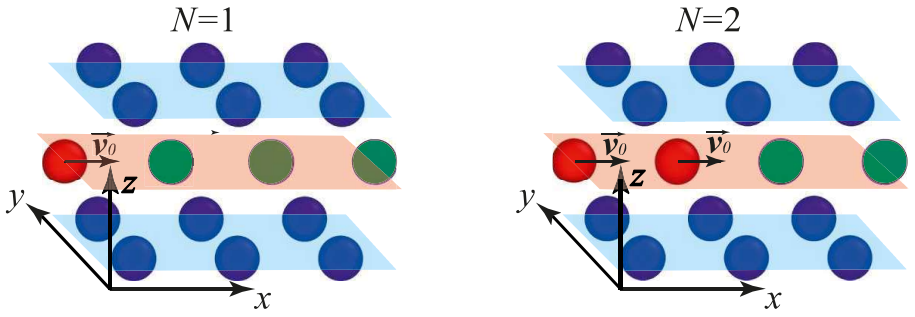

Figure 1. Illustration of the initial conditions for excitation of 1-crowdion (left panel) and 2-crowdion (right panel) by imposing initial velocities to the selected atoms along the $\langle 111 \rangle$ close-packed atomic row in bcc lattice. Only part of the computation cell is shown. The initial velocity v_0 along the x-axis is given to the atoms colored in red. Atoms colored in green are in the close-packed row, where the soliton/crowdion propagates. All other atoms are colored in blue.

W and $a_0 = 3.03$ Å for V. The interatomic distance is $h = a_0\sqrt{3}/2$. One has $h = 2.72$ Å for W and $h = 2.62$ Å for V. The computational cells of W and V contain 82944 atoms and are of the sizes of $391.58 \times 61.53 \times 53.29$ Å and $377.87 \times 59.38 \times 51.42$ Å, respectively. All molecular dynamics simulations are performed at zero initial temperature T=0 K using the NVE (constant number of atoms, volume, and energy) thermodynamic ensemble. The equations of motion are integrated using the Verlet integration scheme with the time step of 0.5 fs.

Excitation of 1- or 2-crowdions is performed by setting an initial directed momentum along the $\langle 111 \rangle$ close-packed direction to one or two neighboring atoms, respectively, according to the scheme illustrated in Fig. 1. The atoms to which the initial momentum is transferred are colored in red. All other atoms in the computational cell have zero initial velocities. Initial displacements of all atoms are equal to zero.

The kinetic energy that is imparted to the crystal at $t = 0$ is

$$T_0 = N\frac{mv_0^2}{2}, \tag{2}$$

where $N = 1$ or 2 is the number of excited atoms, m is the atom mass, v_0 is the initial velocity of the excited atom. In the present study, $m = 183.84$ u for W and $m = 50.941$ u for V.

III. NUMERICAL RESULTS

If the energy of the initial excitation is insufficient to overcome the potential barrier, then the Frenkel pair is not formed and the compressive soliton (focuson) propagates. This localized excitation only transfers energy, but not a mass. Gradually, the energy of the initial excitation dissipates in the lattice, and all atoms return to their equilibrium lattice positions. Usually, the threshold level of an atomic displacement corresponds to a half of the interatomic distance, $h/2 = a_0\sqrt{3}/4$. When the displacement of the excited atom exceeds $h/2$, it does not return to its original equilibrium position, but moves to the next one. This corresponds to crowdion motion, i.e., wave propagation with relay-race motion of interstitial atom in a close-packed atomic rows. Note that both supersonic 1- and 2-crowdions transfer the mass of one interstitial atom and some energy.

In the following sections, we present the results of excitation of focusons or supersonic 1- and 2-crowdions in bcc W and V. Atomic displacements, radiation of energy and crowdion path lengths are analyzed.

A. 1-crowdion

An excitation of one atom in W and V lattices with relatively low initial velocity results in a formation of localized compressive soliton also called focuson. The soliton propagation is illustrated in Figs. 2(a,c) for W and in Figs. 2(b,d) for V, by showing the normalized atomic displacements in the close-packed row, where the soliton moves. When the initial energy is relatively low (top row in Fig. 2), the maximal displacement of atoms is approximately $\Delta x/h \approx 0.5$, and the atoms move back into their initial equilibrium lattice sites. The Frenkel pair is not formed in this case. The soliton moves with supersonic velocity and intensively dissipates its energy into the lattice via phonons. For this reason, the soliton stops after a while, and the traveled distance is rather short. It should be noted that the dynamics of solitons in W and V is noticeably different. Comparison of Figs. 2 (a) and (b) reveals that in V, the atoms return to their equilibrium positions faster, while the atoms in W stay longer at $\Delta x/h \approx 0.5$, which corresponds to the top of the potential barrier. The reason for this difference in the dynamics of solitons in two metals will be explained below.

If the initial velocity is slightly below the threshold level, that is $v_0 = 110$ Å/ps

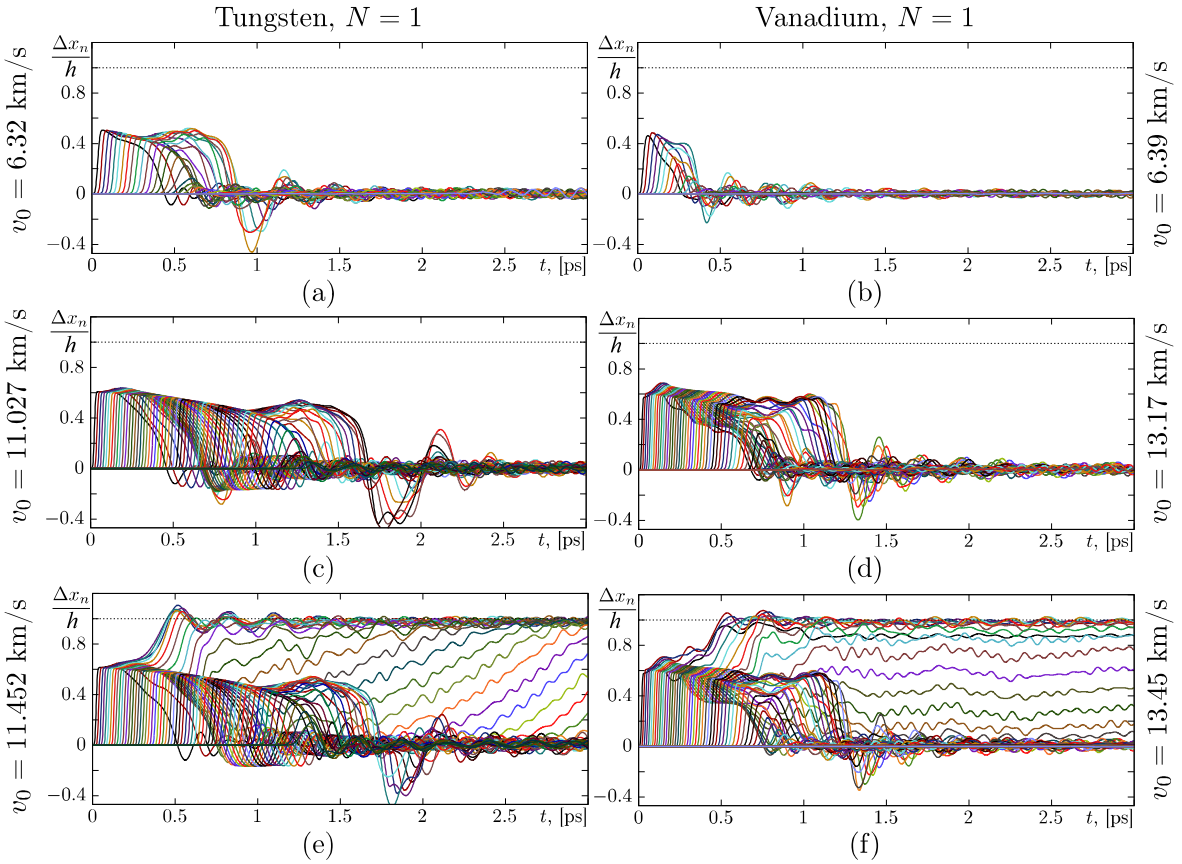

Figure 2. (Color online) The relative atomic displacements $\Delta x/h$ as functions of time illustrating propagation of 1-soliton (a)-(d) and 1-crowdion (e)-(f) in W (left column) and V (right column) at different initial velocities v_0 (kinetic energy T_0): (a) 6.32 km/s (38.9 eV), (b) 6.39 km/s (10.8 eV), (c) 11.0 km/s (119 eV), (d) 13.2 km/s (45.8 eV), (e) 11.5 km/s (128 eV), (f) 13.5 km/s (47.8 eV).

=11.0 km/s (T_0 = 119 eV) for W and v_0 = 132 Å/ps =13.2 km/s (T_0 = 45.8 eV) for V, the distance travelled by the solitons becomes noticeably longer. However, the mass transfer does not occur. This is clearly illustrated in Figs. 2(c) and (d) for both bcc metals. In this case, atoms remain close to their saddle point between the two neighboring lattice sites, which is at $\Delta x/h = 0.5$, during relatively long time. It is worth noting that at a certain time atomic displacements can even exceed $h/2$, but atoms still move back into the initial lattice sites. However, this occurs only when the soliton energy is relatively low and the number of atoms with displacements greater than $h/2$ is relatively small.

An increase of the initial excitation velocity up to v_0 = 11.5 km/s for W and up to v_0 = 13.5 km/s for V results in a formation of a supersonic crowdion. The threshold

value of the excitation energy is $T_0 = 128$ eV for W and $T_0 = 47.8$ eV for V. As clearly seen in Figs. 2(e) and (f), atomic displacements exceed the saddle point (the potential barrier) and atoms start to move into the neighboring lattice sites at $\Delta x/h = 1$. Supersonic crowdion constantly radiates energy and slows down[36]. When the crowdion energy becomes insufficient for supersonic propagation, it evolves into a subsonic crowdion. Supersonic crowdion is localized on one or two atoms, while subsonic crowdion is considerably wider (half a dozen to a dozen atoms) and it can carry the localized mode oscillating at frequency above the phonon spectrum of the lattice[68]. In both W and V, the transition from super- to subsonic regime occurs at the time instant of about $t = 0.6$ ps, see Figs. 2(e) and (f). For $t > 0.6$ ps, propagation of subsonic crowdions is accompanied by the oscillation of atoms' trajectories at the frequency of 11 THz for W and 13 THz for V. Note that these frequencies are considerably higher than the maximal phonon frequency, which is 6.8 THz for W[69] and 8.1 THz for V[53]. Since the vibrational mode localized on subsonic crowdions does not resonate with phonons and does not lose energy to excite them, it has a very long lifetime[68]. The subsonic crowdion in W propagates from left to right, moving atoms from their initial positions into neighboring lattice sites, Fig. 2(e); while in V the subsonic crowdion does not move as demonstrated in Fig. 2(f), since the trajectories of the atoms remain parallel to the abscissa, showing the vibrations mentioned above. In the subsonic regime of motion crowdion in W transfers to the adjacent sites about 5 atoms in 1 ps. The latter means that the propagation velocity is of about $5h$/ps=13.6 Å/ps=1.36 km/s. The velocity of sound in W is 5.2 km/s.

It can be concluded that the threshold values of the initial velocity v_0, when the external excitation creates a supersonic 1-crowdion, are $v_0 \approx 11.5$ km/s ($T_0 = 128$ eV) for W and $v_0 \approx 13.5$ km/s ($T_0 = 47.8$ eV) for V. Deceleration of a supersonic crowdion produces a moving subsonic crowdion in W and standing subsonic crowdion in V. Subsonic crowdions, produced by slowing down supersonic crowdions, carry a localized vibrational mode with a frequency above the phonon spectrum[68].

B. 2-crowdion

A focuson or supersonic 2-crowdion is excited by setting initial velocities v_0 for two neighboring atoms in a close-packed atomic row, as shown in Fig. 1(b). If v_0 is below a

threshold value, a compressive soliton (focuson) is excited. Examples are given in Figs. 3(a) and (b) by applying $v_0 = 3.16$ km/s ($T_0 = 19.5$ eV) for W and $v_0 = 4.46$ km/s ($T_0 = 10.5$ eV) for V, respectively. A few atoms have a maximum displacement greater than $\Delta x/h = 0.5$, but this is not enough to create a Frenkel pair. After the energy transferred to the crystal is dissipated through the lattice, all atoms return to their original lattice sites. The atomic displacement curves have a specific 'two-step' shape stipulated by the excitation of 2 adjacent atoms.

An increase of the initial velocity up to $v_0 = 3.61$ km/s ($T_0 = 25.4$ eV) for W and $v_0 = 4.91$ km/s ($T_0 = 12.7$ eV) for V results in an overcoming of the potential barrier and in the formation of a supersonic 2-crowdion. This case is represented in Figs. 3(c) and (d) for W and V, respectively. It is seen that the atoms shift in two steps by $\Delta x/h \approx 0.75$ and thereafter slowly move towards adjacent lattice sites. At the same time, the supersonic stage in these cases is rather short; it ends approximately at $t = 0.5$ ps for both metals. For $t > 0.5$ ps energy of the crowdion becomes lower than a certain threshold level, and the supersonic crowdion transforms into a subsonic one. In W the subsonic crowdion continues its motion from the left to the right bearing a localized vibrational mode of relatively small amplitude. In V the subsonic crowdion does not move, since the curves $\Delta x_n(t)$ are parallel to the time axis, see Fig. 3(d). These curves show oscillations at a relatively large amplitude. The frequency of these oscillations can be estimated as 14 THz, which is above the upper edge of the phonon spectrum of V (8.1 THz). This explains why the oscillations decay very slowly: they do not resonate with phonons and do not waste energy on their excitation.

Supersonic 2-crowdions propagating longer distances can be seen in Figs. 3(e) and (f). They were excited in W and V with $v_0 = 5.83$ km/s ($T_0 = 66.2$ eV) and $v_0 = 6.39$ km/s ($T_0 = 21.6$ eV), respectively. In this case, the atoms in two steps move to the adjacent lattice sites at $\Delta x_n/h = 1.0$. Let the time interval between the neighboring $\Delta x_n/h$ curves is Δt. Then the crowdion speed is $h/\Delta t$. The sound velocity in W, as mentioned above, is 52 Å/ps. For this velocity $\Delta t = 0.052$ ps. As can be seen in Fig. 3(e), the supersonic stage of crowdion propagation in W is relatively long and lasts till 1.5 ps. Similar calculations for V give the supersonic regime of motion till 0.5 ps.

Comparison of Figs. 3(e) and (f) reveals that in W the transition from supersonic to subsonic propagation is smooth, while it is abrupt in V. This explains why the just born subsonic crowdion moves in W, but not in V, as well as why the oscillation mode localized

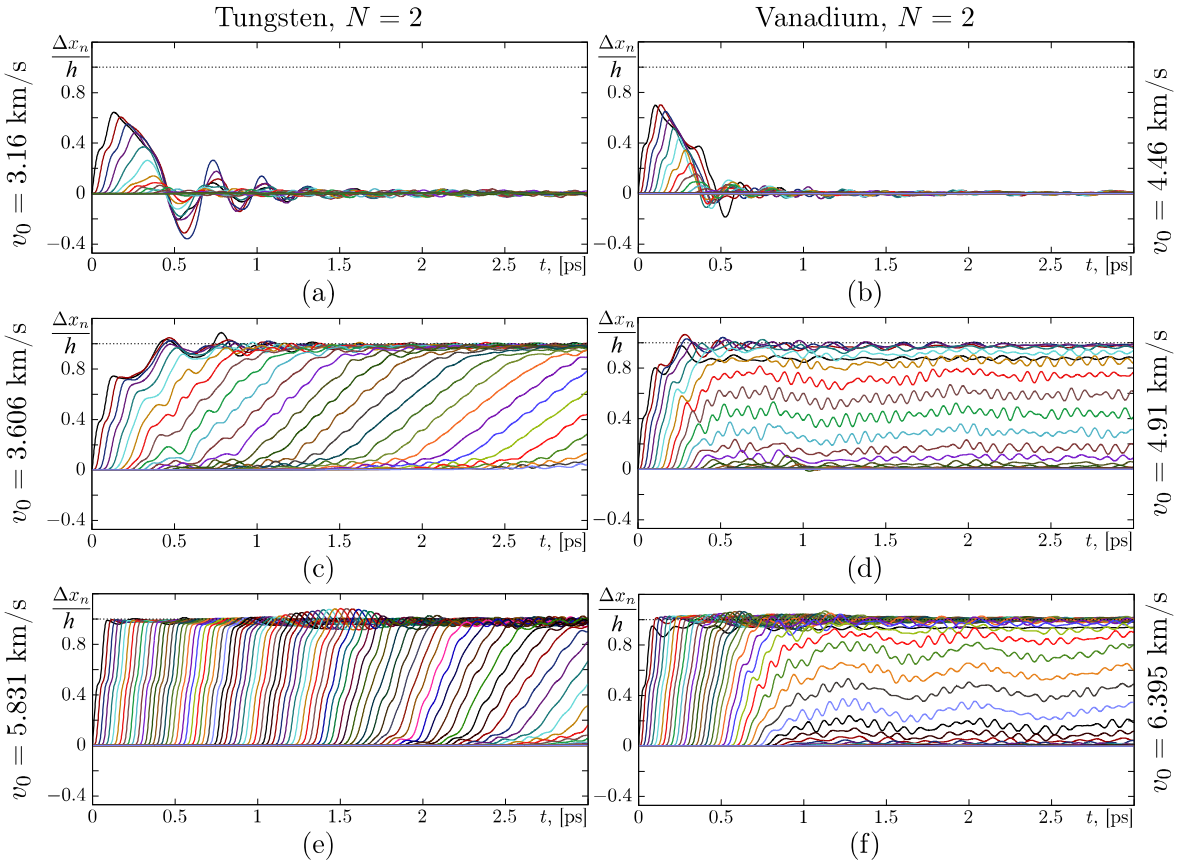

Figure 3. (Color online) The relative atomic displacements $\Delta x/h$ as functions of time illustrating propagation of 2-soliton (a)-(b) and 2-crowdion (c)-(f) in W (left column) and V (right column) at different velocities v_0 (kinetic energy T_0): (a) 3.16 km/s (19.5 eV), (b) 4.46 km/s (10.5 eV), (c) 3.61 km/s (25.4 eV), (d) 4.91 km/s (12.7 eV), (e) 5.83 km/s (66.2 eV), (f) 6.39 km/s (21.6 eV).

on subsonic crowdion in V has much higher amplitude than in W. A smooth transition from supersonic to subsonic motion in W ensures the transfer of momentum of the directed motion to the atoms moving along the close-packed row in the subsonic regime. A sharp transition in V leads to the transfer of the energy of the directed motion of the supersonic crowdion to a large-amplitude vibrational mode localized on the subsonic crowdion.

An excitation of supersonic 2-crowdion needs noticeably lower initial energy as compared to supersonic 1-crowdion. Recall that the minimal energy required for excitation of a supersonic 1-crowdion is 128 eV in W and 47.8 eV in V. On the other hand, for excitation of supersonic 2-crowdions it is sufficient to spend 25.4 eV in W and 12.7 eV in V. The energy gain is 5 times for W and 3.8 times for V. Since both the supersonic 1- and 2-crowdions

each carry one interstitial atom, it can be concluded that the supersonic 2-crowdion in bcc crystals is a much more efficient mass transfer mechanism in comparison with the supersonic 1-crowdion.

This effect is described here for the first time for bcc metals. Despite the fact that similar results were obtained earlier for the two-dimensional triangular lattice modeled with the pair-wise Morse interatomic potential[38]. In particular, it was established that the excitation energies of supersonic 2-crowdion are two times less than that for supersonic 1-crowdion. Note that similar results have been obtained in Ref.[36], where the authors have found that excitation of 2×1 supersonic crowdion cluster costs 2.4 and 3 times more energy than that for 2×2 and 2×4 supersonic crowdion clusters, respectively.

C. Evolution of crowdion energy

In Fig. 4, temporal evolution of the kinetic energy $T_n(t)$ of the n-th atom in the close-packed row in W is plotted for (a) 1-crowdion and (b) 2-crowdion. The crowdions were excited with $v_0 = 11.5$ km/s ($T_0 = 128$ eV) in (a) and $v_0 = 5.83$ km/s ($T_0 = 66.2$ eV) in (b). The maximal value of the kinetic energy of atoms can be regarded as the maximal kinetic energy of crowdion. For 1-crowdion, the maxima of the energies are well fitted by a cubic polynomial with inaccuracy less than 1%. In 2-crowdion, two atoms simultaneously have a high kinetic energy. The envelop function for the maximal kinetic energy of atoms decreases in time for the 2-crowdion almost linearly (the envelopes are shown in Fig. 4 as solid red lines).

The result presented in Fig. 4 demonstrates that the energy of the 1-crowdion decreases with time faster than the energy of the 2-crowdion. This can be explained by the fact that collisions of atoms in a 1-crowdion occur at higher energies, which leads to a greater energy dissipation by the lattice. In a 2-crowdion, the energy is shared between two atoms, and the collisions of the atoms occur at a lower energy, resulting in a slower loss of energy by the crowdion.

The envelop functions of the maximal kinetic energy $T(t)$ for (a) W and (b) V are shown in Fig. 5. Initial parameters are specified for each curve in the legends. Curves 1 to 3 are for $N = 1$, while curves 4 and 5 are for $N = 2$. In particular, curves 1 in Fig. 5 correspond to the 1-solitons excited with the low initial energy, see Figs. 2(a) and (b). Curves 2 and 3 in Fig. 5

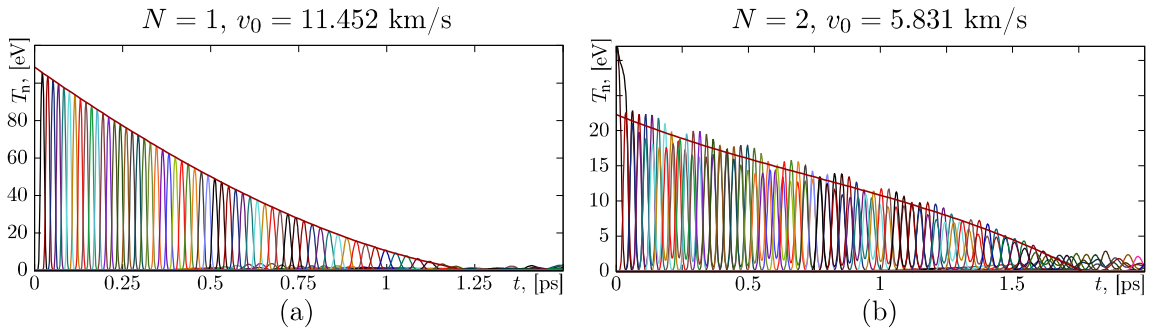

Figure 4. (Color online) Temporal evolution of the kinetic energy $T_n(t)$ of the n-th atom in the close-packed row in W for (a) $N = 1$, $v_0 = 11.5$ km/s ($T_0 = 128$ eV), and (b) $N = 2$, $v_0 = 5.83$ km/s ($T_0 = 66.2$ eV). The envelope lines are shown in red. In (a), it is a cubic polynomial, and in (b) the envelope is almost a linear function.

are for the 1-solitons excited with the sub- and over-threshold energies, see Figs. 2(c),(d) and (e),(f), respectively. Dependencies $T(t)$ for 2-crowdions are noticeably different from those for 1-crowdions. The energy evolution for 2-crowdion induced with the initial energy slightly above the threshold level is shown in Fig. 5 by the curves 4, see Figs. 3(c) and (d). The case of the long-lived 2-crowdion is illustrated in Fig. 5 by the curves 5, see Figs. 3(e) and (f).

As seen in Figs. 5(a) and (b) that curves 1 for 1-solitons in both bcc metals start at relatively low energy level and decay quickly. Curves 2 and 3 start at considerably higher energy level, and then they also decay quickly. Curves 4 for the 2-crowdion excited with the energy slightly above the threshold level have two maxima. The second maximum appears after the transition from the supersonic to subsonic crowdion. The slowly decaying curves 5 in Fig. 5 show $T(t)$ for the long-lived 2-crowdions. The energy level for these curves is relatively low.

Time derivatives of the maximal kinetic energy envelops, dT/dt, characterizing the energy dissipation rate are depicted in Fig. 5 for W (c) and V (d). The energy loss for 2-crowdion is significantly lower than that for 1-crowdion. Moreover, the energy dissipation of 2-crowdion excited with the larger momentum (curves 5) is lower than that for 2-crowdion excited with smaller momentum (curves 4). Curve 5 in Fig. 5(c) is almost horizontal, showing that, as mentioned above, the maximum kinetic energy for a supersonic 2-crowdion in W decreases almost linearly with time.

D. Propagation of supersonic crowdions

Further an analysis of the distance L_s travelled by 1- and 2-crowdions during their supersonic motion as well as the duration of the supersonic stage t_s as functions of the initial velocity v_0 and the initial energy T_0 are presented in Fig. 6. It is clearly seen that in both bcc metals supersonic 2-crowdion covers larger distance and moves longer time as compared to supersonic 1-crowdion excited with the same initial velocity or energy. For comparison, a supersonic 2-crowdion induced in W with $T_0 \approx 70$ eV passes the distance of $L_s = 100$ Å in

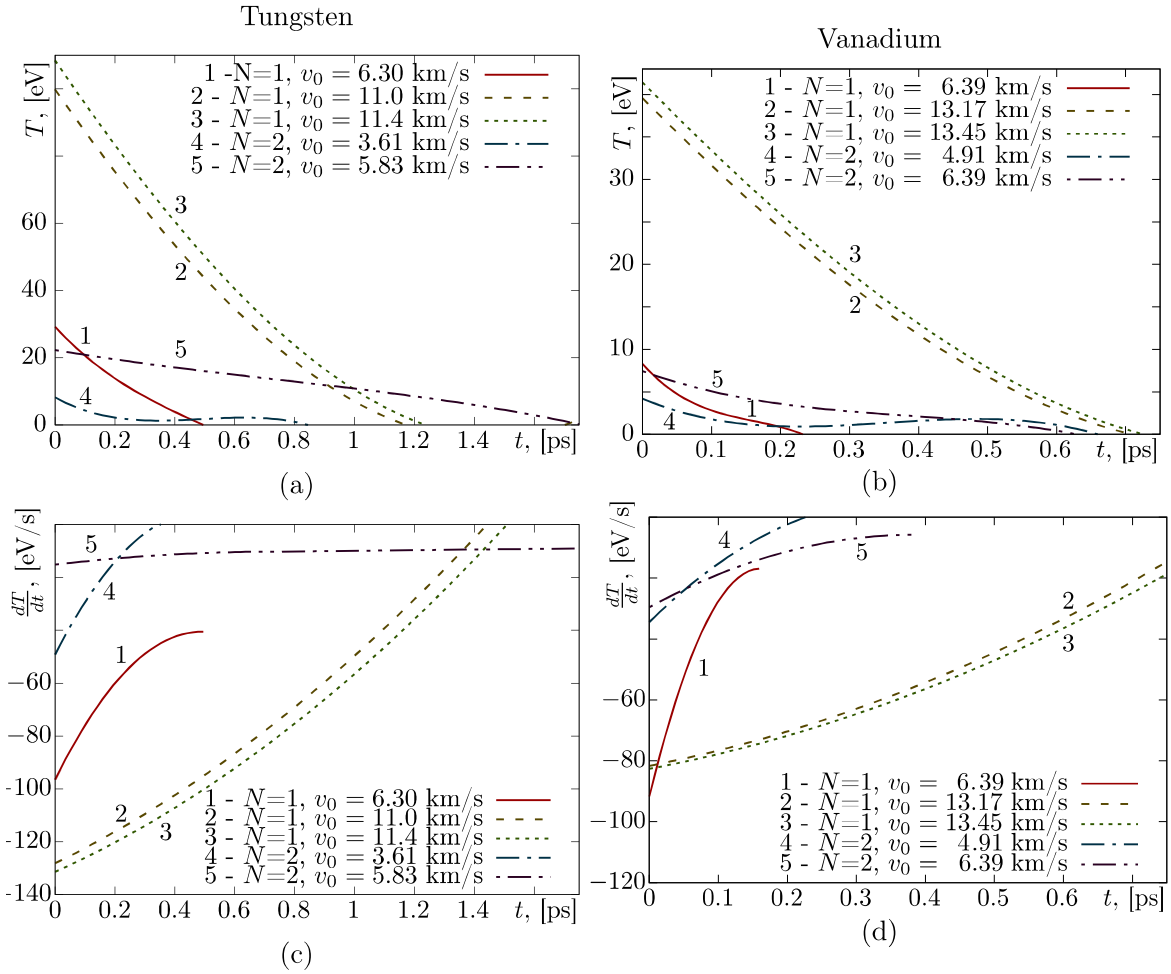

Figure 5. (Color online) (a,b) Envelop functions, $T(t)$, approximating evolution of the maximal kinetic energy of atoms; (c,d) the energy dissipation rate, dT/dt, of the solitons/crowdions as the function of time for W (c) and V (d). Initial parameters are specified for each curve in the corresponding legends.

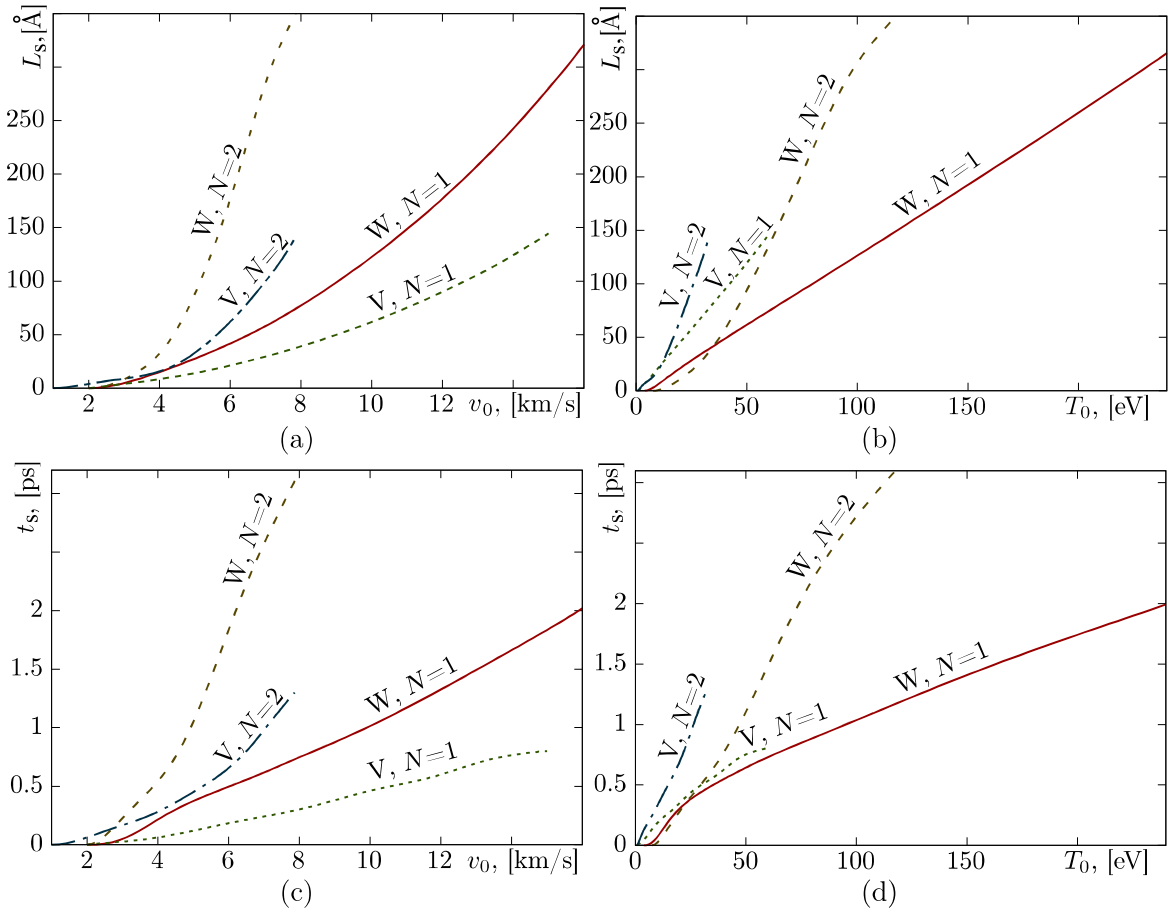

Figure 6. (Color online) (a,b) Propagation distance L_s and (c,d) propagation time t_s of 1- and 2-crowdions with the supersonic velocity in W and V as the functions of the initial velocity v_0 (a,c) and the initial energy T_0 (b,d). The metal and the type of crowdion are indicated in each curve.

$t_s \approx 2$ ps. A supersonic 1-crowdion travels the same distance in $t_s \approx 1.3$ ps being excited at a much higher energy of $T_0 \approx 155$ eV. It should be noted that the dependence $L_s(T_0)$ is almost linear for 1-crowdion and it increases much faster than for 2-crowdion in both studied bcc metals suggesting that 2-crowdions are more efficient at transferring mass. Interestingly, the distance and duration of supersonic propagation of both 1- and 2-crowdions are significantly longer in W than in V.

E. Comparison of interatomic potentials for W and V

It follows from the presented results that supersonic 1- and 2-crowdions propagate much longer distances and need for their excitation lower energies in W than in V. There is also

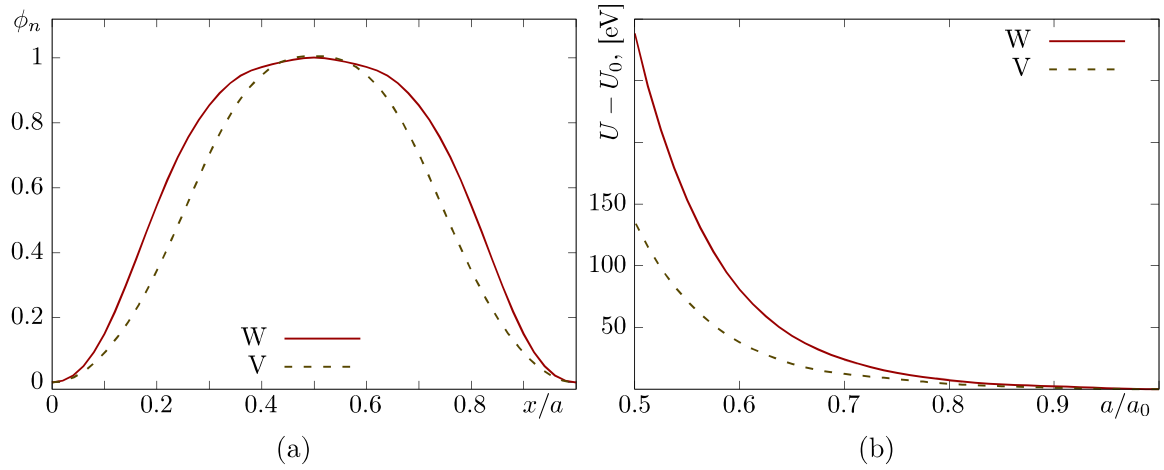

Figure 7. (Color online) (a) Normalized potential function, $\phi_n(x/h)$, defined by Eq. (3); (b) sublimation energy per atom U relative to its equilibrium value, U_0, as the function of the bcc lattice parameter a normalized to its equilibrium value a_0. Results for W are shown by the solid red line and for V by the dashed black line.

a qualitative difference in the transition from supersonic to subsonic crowdion motion in W and V.

These effects cannot be explained by the greater mass and, consequently, the greater kinetic energy of W atoms as compared to V atoms. This is so because the mass of an atom can be taken as a unit for any pure metal with an appropriate choice of the unit of time. Then the explanation of the qualitative difference in the dynamics of crowdions in the two studied bcc metals should be related to the difference in their interatomic interactions.

In order to compare the potentials for W and V, we consider a close-packed atomic row oriented along the x-axis and calculate the potential energy per atom of the row, $\tilde{\phi}_n$, as the function of the rigid shift along the x-axis in the rigid crystal matrix. The function $\tilde{\phi}_n(x)$ has period equal to the interatomic distance h and its minimal and maximal values are $\phi_{\min}$ and $\phi_{\max}$. For quantitative comparison, the potential functions for W and V are presented in Fig. 7(a) in the following normalized form:

$$\phi_n(x/h) = \frac{\tilde{\phi}(x/h) - \phi_{\min}}{\phi_{\max} - \phi_{\min}}. \tag{3}$$

When an atom is moved by a supersonic crowdion along a close-packed row, it overcomes a potential barrier with a height close to $\phi_{\max} - \phi_{\min}$ because the surrounding atoms of the matrix have a very short time to relax and to modify this potential.

It is seen in Fig. 7(a) that the potential profiles are noticeably different. The potential for W, compared to the potential for V, has a narrower minimum and a wider maximum. This difference in potential energy profiles probably explains why the transition from supersonic to subsonic motion is smooth in W and abrupt in V. This leads to the transformation of supersonic crowdions into moving subsonic crowdions in W and standing subsonic crowdions in V. A sharp transition to the subsonic regime in V creates a high-amplitude vibrational mode localized on the subsonic crowdion.

An interesting insight into the structure of the dislocation core in bcc metals can be obtained within the framework of the multi-string Frenkel-Kontorova model[70].

Effect of interatomic potentials on mass transfer by supersonic 2-crowdions was studied in a triangular two-dimensional lattice with Morse and Born-Mayer potentials[37]. It was shown that the potential with a stronger repulsive part promotes self-focusing collisions of atoms and, consequently, the propagation of supersonic crowdions.

In order to compare the repulsive parts of the potentials for W and V we calculate the sublimation energy per atom U as the function of the lattice parameter a. In Fig. 7(b) the difference $U - U_0$ as the function of a/a_0 is plotted, where U_0 is the sublimation energy at $a = a_0$, where a_0 is the equilibrium lattice parameter. The result is presented in Fig. 7(b) for the range of $0.5 < a/a_0 < 1.0$, since this is the range of self-focusing atomic collisions[38]. If the distance between colliding atoms becomes smaller than the half of the equilibrium interatomic distance, then the collisions are defocusing and propagation of a supersonic crowdion is impossible. That is why stable (self-focusing) propagation of supersonic crowdions is possible only if the collision velocity of the atoms is not too high. Besides, this is the reason why the supersonic 2-crowdions are much more efficient in mass transfer in comparison with the supersonic 1-crowdions. In 2-crowdion the energy is shared by the two atoms moving simultaneously with the high velocity and collision velocities are smaller than that in 1-crowdion with the same energy.

The result presented in Fig. 7(b) shows that the compressive part of the potential in W is much stronger than in V. This explains the fact that the supersonic motion of crowdions in W is noticeably longer in duration and distance in comparison with V. Indeed, self-focusing propagation in W is possible for higher energy atoms, and they can travel longer distances. In addition to that, it should be noted that a detailed analysis of large statistics of molecular dynamics simulations was performed with different embedded atom method potentials for

Fe and W in Refs.[71,72].

F. Effect of temperature

Temperature is an important parameter when discussing the motion of interstitial atoms[6,71]. Figure 8 shows the effect of temperature on the propagation distance of a supersonic 2-crowdion in W. The propagation distance is normalized to the interatomic distance. Two initial velocities of the excited atoms $v_0 = 5.7$ and 7.8 km/s (blue and black lines, respectively) are considered. The temperature range from 300 to 1300 K covers temperatures that are important for the application of W. Each point on the plot is the result of averaging over five realizations.

As seen in Fig. 8, an increase in temperature leads to a decrease in the crowdion propagation distance. The decrease is fast at low temperatures and becomes slower as temperature increases. At high temperatures, the propagation distance of a supersonic 2-crowdion is about ten interatomic distances. Then the structure of the supersonic 2-crowdion is destroyed, and its energy is given to the formation of supersonic 1-crowdions moving in directions different from the direction of the initial momentum.

G. Effect of interatomic potentials for W

It is well-known that interatomic potentials influence the results of molecular dynamics simulations, especially for simulations of high-energy interatomic collisions. So far, the results for the interatomic potential by Marinica *et al.*[67] were reported. Recently, Mason *et al.* have developed interatomic potential for W that is particularly well suited for modeling vacancy-type defects[73]. Figure 9 shows the result of application of this potential for simulation of supersonic 1- and 2-crowdions. The left (right) column is for $N = 1$ ($N = 2$). For each panel, the initial velocity of the atoms is indicated.

Panels (a) and (c) of Fig. 9 should be compared to Fig. 2, panels (c) and (e) respectively, since they are plotted for 1-crowdion ($N = 1$) and for the same initial velocities. Similarly, panels (b) and (d) of Fig. 9 are plotted for 2-crowdion ($N = 2$) and the same initial velocities as in Fig. 3, panels (c) and (e), respectively. Comparison reveals that the potential by Mason *et al.*[73] predicts even greater propagation distances for supersonic crowdions than the

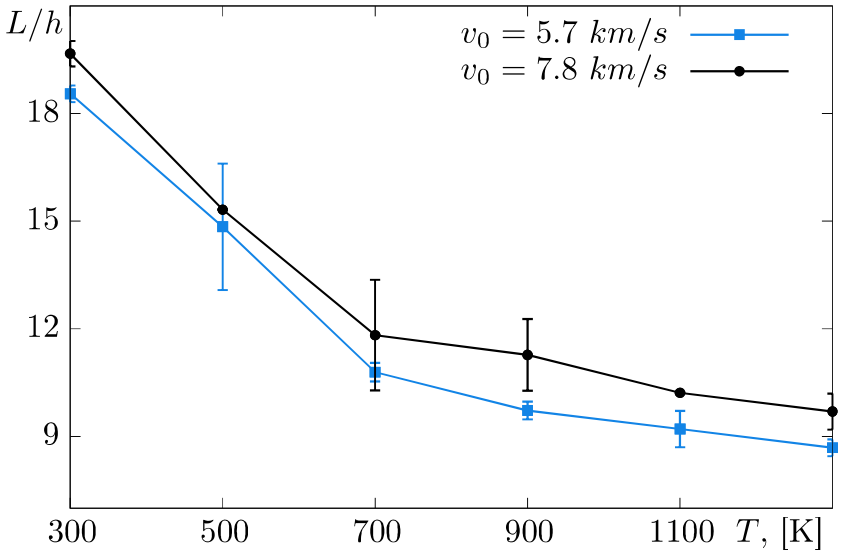

Figure 8. The effect of temperature on the propagation distance of the supersonic 2-crowdion in W. The 2-crowdions are excited with the initial velocities of 5.7 km/s (blue line, blue square dots) and 7.8 km/s (black line, route dots). Each point is the result of averaging over five realizations. Error bars represent the variability of travelled distances. Lines connecting the data points are visual guides.

potential by Marinica *et al.*[67]. This result confirms that the repulsive part of the potentials must be carefully adjusted to better describe collisions of high-energy atoms[71].

IV. CONCLUSIONS AND FUTURE WORK

In the present study, for the first time, the dynamics of N-solitons/N-crowdions (N is a number of initially excited neighboring atoms in one close-packed atomic row) were investigated in bcc metals W and V via molecular dynamics simulations. The main conclusions can be drawn as follows.

- In order to initiate mass transfer by a supersonic 1-crowdion, an energy of 128 eV in W and 47.8 eV in V is required. On the other hand, to initiate mass transfer by a supersonic 2-crowdion, it is sufficient to expend an energy of 25.4 eV in W and 12.7 eV in V, i.e., 5 and 3.8 times less, respectively. Less energy is not enough to create a Frenkel pair and a compressive soliton (focuson) is formed, which does not transfer mass.

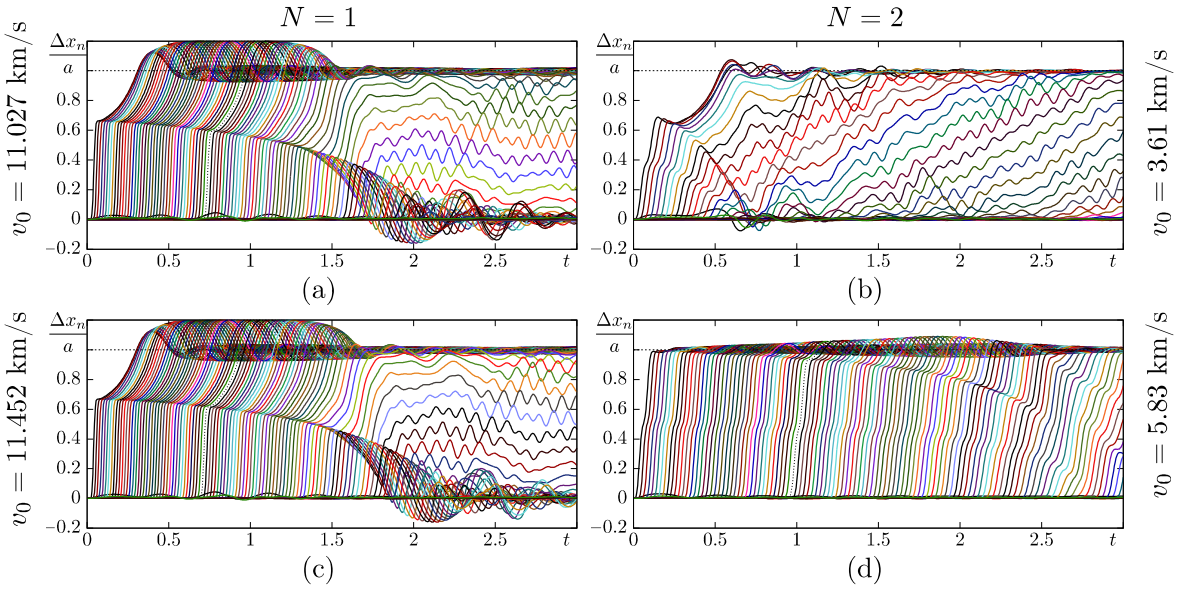

Figure 9. (Color online) The relative atomic displacements $\Delta x/h$ as the functions of time illustrating propagation of 1-crowdion (a), (c) and 2-crowdion (b), (d) in W calculated for a new interatomic potential by Mason *et al.*[73] at different initial velocities v_0 (kinetic energy T_0): (a) 11.027 km/s (119 eV) (compare with Fig. 2(c)), (b) 3.61 km/s (25.4 eV) (Fig. 3(c)), (c) 11.452 km/s (128 eV) (Fig. 2(e)), (d) 5.83 km/s (66.2 eV) (Fig. 3(e)).

- Energy dissipation rate for supersonic 2-crowdion is significantly lower than that for supersonic 1-crowdion. This can be explained by the fact that collisions of atoms in a supersonic 1-crowdion, having the same energy as supersonic 2-crowdion, occur at higher velocities, which leads to a greater energy dissipation by the lattice. In a supersonic 2-crowdion, the energy is shared between two atoms, and the collisions of the atoms occur at a lower velocity, resulting in a slower loss of energy by the crowdion.

- Deceleration of a supersonic crowdion produces a moving subsonic crowdion in W and standing subsonic crowdion in V. Subsonic crowdions, produced by slowing down supersonic crowdions, carry a localized vibrational mode with a frequency above the phonon spectrum.

- In W the transition from supersonic to subsonic regime is smooth, while it is abrupt in V. This explains why the just born subsonic crowdion moves in W, but not in V. A smooth transition from supersonic to subsonic motion in W ensures the transfer of

momentum of the directed motion to the atoms moving along the close-packed row in the subsonic regime. A sharp transition in V leads to the transfer of the energy of the directed motion of the supersonic crowdion to a large-amplitude vibrational mode localized on the subsonic crowdion. This explains why the oscillation mode localized on subsonic crowdion in V has much higher amplitude than in W.

- The potential for W, compared to the potential for V, has a narrower minimum and a wider maximum. This difference in potential energy profiles probably explains the reason why the transition from supersonic to subsonic motion is smooth in W and abrupt in V.

- Interatomic interactions in W have a much stronger repulsive part as compared to V, which facilitates the self-focusing propagation of supersonic crowdions in W.

In this work, we mainly discussed the supersonic stage of crowdion motion, since only in the supersonic regime 1- and 2-crowdions are different. Both of them carry one interstitial atom each and after the transition to the subsonic regime they become indistinguishable. However, interstitial atoms continue their directed motion after the transition from supersonic to subsonic regime. An open question stands: do supersonic 2-crowdions form in collision cascades, and if so, how many of them compared to the number of supersonic 1-crowdions? Since, as already noted, both types of supersonic crowdions carry a single interstitial atom, their dynamics must be carefully analyzed to distinguish them.

Starting with the work of Heinisch and Singh[74], the object kinetic Monte Carlo (OKMC) method has been developed[75–77] to understand the evolution of microstructure in materials under irradiation. The main advantage of this method is that it allows one to analyze time and space scales that are inaccessible to the molecular dynamics method. In OKMC method, defects and defect clusters perform random walks imitating their diffusion motion and interact with each other, simulating the transformation and relaxation of the structure. In the present work, we have analyzed the supersonic rather than diffusive motion of self-interstitial atoms. This type of motion of point defects can be incorporated in the OKMC method to describe the collisional stage of cascade development.

The results of our study contribute to a better understanding of the supersonic motion of crowdions in metals and pose new problems that should be solved in future work. A comparative analysis of the dynamics of supersonic crowdions should be carried out for

other metals which are planned to be operated under extreme conditions and which are important for nuclear power engineering. In order to verify the results obtained by molecular dynamics, it is necessary to analyze the supersonic motion of 1- and 2-crowdions in bcc metals using more accurate *ab initio* methods, as was done for fcc Al[28]. A recent study of supersonic $M \times N$-crowdions in a two-dimensional triangular Morse lattice, where $M \times N$ is a block of excited atoms, showed that the distances traveled at supersonic speed significantly exceed those for supersonic 1-crowdions[36]. For bcc and fcc metals, the class of supersonic $M \times N \times K$-crowdions has not yet been investigated at all and therefore should be analysed. Propagation of supersonic crowdion clusters can produce in the lattice delocalized vacancies (voidions) moving along a close-packed atomic row at subsonic or supersonic speed[36,78–83]. These objects deserve further study in various metals and alloys. In addition, real materials have various kinds of defects and are characterized by an increased concentration of vacancies upon irradiation. In our future work, we are going to study the influence of various types of crystal lattice defects on the dynamics of crowdions.

V. ACKNOWLEGEMENTS

K.E.A. and I.A.Sh. acknowledge the financial support of the Russian Science Foundation, grant No. 21-12-00275.

---

* igor_sar@li.ru

† dmitry.bachurin@kit.edu

‡ elena.a.korznikova@gmail.com

§ dmitriev.sergey.v@gmail.com

[1] A. M. Kiss, A. Y. Fong, N. P. Calta, V. Thampy, A. A. Martin, P. J. Depond, J. Wang, M. J. Matthews, R. T. Ott, C. J. Tassone, et al., Laser-induced keyhole defect dynamics during metal additive manufacturing, Advanced Engineering Materials 21 (10) (2019) 1900455.

[2] E. Korznikova, E. Schafler, G. Steiner, M. J. Zehetbauer, Measurements of vacancy type defects in SPD deformed Ni, TMS Annual Meeting 2006 (2006) 97–102.

[3] Q. Wei, B. E. Schuster, S. N. Mathaudhu, K. T. Hartwig, L. J. Kecskes, R. J. Dowding, K. T. Ramesh, Dynamic behaviors of body-centered cubic metals with ultrafine grained and nanocrystalline microstructures, Materials Science and Engineering: A 493 (1-2) (2008) 58–64.

[4] I. A. Shepelev, A. P. Chetverikov, S. V. Dmitriev, E. A. Korznikova, Shock waves in graphene and boron nitride, Computational Materials Science 177 (2020) 109549.

[5] D. A. Terentyev, T. P. C. Klaver, P. Olsson, M.-C. Marinica, F. Willaime, C. Domain, L. Malerba, Self-trapped interstitial-type defects in iron, Physical Review Letters 100 (14) (2008) 145503.

[6] D. A. Terentyev, L. Malerba, M. Hou, Dimensionality of interstitial cluster motion in bcc-Fe, Physical Review B 75 (10) (2007) 104108.

[7] Z. Zhang, K. Yabuuchi, A. Kimura, Defect distribution in ion-irradiated pure tungsten at different temperatures, Journal of Nuclear Materials 480 (2016) 207–215.

[8] W. H. Zhou, C. G. Zhang, Y. G. Li, Z. Zeng, Transport, dissociation and rotation of small self-interstitial atom clusters in tungsten, Journal of Nuclear Materials 453 (1-3) (2014) 202–209.

[9] F. Granberg, J. Byggmästar, K. Nordlund, Molecular dynamics simulations of high-dose damage production and defect evolution in tungsten, Journal of Nuclear Materials 556 (2021). doi:10.1016/j.jnucmat.2021.153158.

[10] Z.-Z. Li, Y.-H. Li, D. Terentyev, N. Castin, A. Bakaev, G. Bonny, Z. Yang, L. Liang, H.-B. Zhou, F. Gao, G.-H. Lu, Investigating the formation mechanism of void lattice in tungsten under neutron irradiation: from collision cascades to ordered nanovoids, Acta Materialia 219 (2021). doi:10.1016/j.actamat.2021.117239.

[11] H. Nordmark, R. Holmestad, J. C. Walmsley, A. Ulyashin, Transmission electron microscopy study of hydrogen defect formation at extended defects in hydrogen plasma treated multicrystalline silicon, Journal of Applied Physics 105 (3) (2009) 033506.

[12] H. R. Paneth, The mechanism of self-diffusion in alkali metals, Phys. Rev. 80 (4) (1950) 708–711. doi:10.1103/PhysRev.80.708.

[13] P. M. Derlet, D. Nguyen-Manh, S. L. Dudarev, Multiscale modeling of crowdion and vacancy defects in body-centered-cubic transition metals, Physical Review B 76 (5) (2007) 054107.

[14] U. Bhardwaj, A. Sand, M. Warrier, Graph theory based approach to characterize self interstitial defect morphology, Computational Materials Science 195 (2021). doi:10.1016/j.commatsci.2021.110474.

[15] A. Xu, D. E. J. Armstrong, C. Beck, M. P. Moody, G. D. W. Smith, P. A. J. Bagot, S. G. Roberts, Ion-irradiation induced clustering in W-Re-Ta, W-Re and W-Ta alloys: An atom probe tomography and nanoindentation study, Acta Materialia 124 (2017) 71–78.

[16] K. Xu, M. H. Weber, Y. Cao, W. Jiang, D. J. Edwards, B. R. Johnson, J. S. McCloy, Ion irradiation induced changes in defects of iron thin films: Electron microscopy and positron annihilation spectroscopy, Journal of Nuclear Materials 526 (2019) 151774.

[17] D. R. Mason, A. E. Sand, X. Yi, S. L. Dudarev, Direct observation of the spatial distribution of primary cascade damage in tungsten, Acta Materialia 144 (2018) 905–917. doi:10.1016/j.actamat.2017.10.031.

[18] J. Fang, L. Liu, N. Gao, W. Hu, H. Deng, Molecular dynamics simulation of the behavior of typical radiation defects under stress gradient field in tungsten, Journal of Applied Physics 130 (12) (2021). doi:10.1063/5.0059748.

[19] J. Wang, Q. Hou, B. L. Zhang, Migration behavior of self-interstitial defects in tungsten and iron, Solid State Communications 325 (2021). doi:10.1016/j.ssc.2020.114158.

[20] B. Q. Fu, S. P. Fitzgerald, Q. Hou, J. Wang, M. Li, Effect of collision cascades on dislocations in tungsten: A molecular dynamics study, Nuclear Instruments and Methods in Physics Research, Section B: Beam Interactions with Materials and Atoms 393 (2017) 169–173. doi:10.1016/j.nimb.2016.10.028.

[21] F. J. Domínguez-Gutiérrez, J. Byggmästar, K. Nordlund, F. Djurabekova, U. von Toussaint, On the classification and quantification of crystal defects after energetic bombardment by machine learned molecular dynamics simulations, Nuclear Materials and Energy 22 (2020). doi:10.1016/j.nme.2019.100724.

[22] A. Chartier, M.-C. Marinica, Rearrangement of interstitial defects in alpha-fe under extreme condition, Acta Materialia 180 (2019) 141–148. doi:10.1016/j.actamat.2019.09.007.

[23] J. Fu, Y. Chen, J. Fang, N. Gao, W. Hu, C. Jiang, H.-B. Zhou, G.-H. Lu, F. Gao, H. Deng, Molecular dynamics simulations of high-energy radiation damage in w and w–re alloys, Journal of Nuclear Materials 524 (2019) 9–20. doi:10.1016/j.jnucmat.2019.06.027.

[24] J. Wang, B. He, W. Song, W. Dang, Energetics, kinetics and dynamics of self-interstitial clusters in bcc tungsten, Molecular Simulation 45 (8) (2019) 666–671. doi:10.1080/08927022.2019.1578356.

[25] F. Cheng, Q. Zheng, Y. Li, C. Zhang, Z. Zeng, Electronic energy loss assessment in theoretical modeling of primary radiation damage in tungsten, International Journal of Modern Physics C 32 (10) (2021). doi:10.1142/S0129183121501345.

[26] N. Castin, A. Bakaev, G. Bonny, A. E. Sand, L. Malerba, D. Terentyev, On the onset of void swelling in pure tungsten under neutron irradiation: An object kinetic monte carlo approach, Journal of Nuclear Materials 493 (2017) 280–293. doi:10.1016/j.jnucmat.2017.06.008.

[27] S. L. Dudarev, P.-W. Ma, Elastic fields, dipole tensors, and interaction between self-interstitial atom defects in bcc transition metals, Physical Review Materials 2 (3) (2018). doi:10.1103/PhysRevMaterials.2.033602.

[28] E. A. Korznikova, V. V. Shunaev, I. A. Shepelev, O. E. Glukhova, S. V. Dmitriev, Ab initio study of the propagation of a supersonic 2-crowdion in fcc Al, Computational Materials Science 204 (2022) 111125. doi:10.1016/j.commatsci.2021.111125.

[29] M. R. Gilbert, K. Arakawa, Z. Bergstrom, M. J. Caturla, S. L. Dudarev, F. Gao, A. M. Goryaeva, S. Y. Hu, X. Hu, R. J. Kurtz, A. Litnovsky, J. Marian, M.-C. Marinica, E. Martinez, E. A. Marquis, D. R. Mason, B. N. Nguyen, P. Olsson, Y. Osetskiy, D. Senor, W. Setyawan, M. P. Short, T. Suzudo, J. R. Trelewicz, T. Tsuru, G. S. Was, B. D. Wirth, L. Yang, Y. Zhang, S. J. Zinkle, Perspectives on multiscale modelling and experiments to accelerate materials development for fusion, Journal of Nuclear Materials 554 (2021). doi:10.1016/j.jnucmat.2021.153113.

[30] P.-W. Ma, D. R. Mason, S. L. Dudarev, Multiscale analysis of dislocation loops and voids in tungsten, Physical Review Materials 4 (10) (2020). doi:10.1103/PhysRevMaterials.4.103609.

[31] S. L. Dudarev, D. R. Mason, E. Tarleton, P.-W. Ma, A. E. Sand, A multi-scale model for stresses, strains and swelling of reactor components under irradiation, Nuclear Fusion 58 (12) (2018). doi:10.1088/1741-4326/aadb48.

[32] C. Becquart, A. Souidi, M. Hou, Replacement collision and focuson sequences revisited by full molecular dynamics and its binary collision approximation, Philosophical Magazine 85 (4-7 SPEC. ISS.) (2005) 409–415. doi:10.1080/02678370412331320251.

[33] V. Natsik, S. Smirnov, Dislocations and crowdions in two-dimensional crystals. Part III: Plastic deformation of the crystal as a result of defect movement and defect interaction with the field of elastic stresses, Low Temp. Phys. 42 (3) (2016) 207–218. doi:10.1063/1.4945583.

[34] S. A. Starikov, A. R. Kuznetsov, V. V. Sagaradze, Crowdion in deformed fcc metal. atomistic modeling, Physics of Metals and Metallography 122 (12) (2021) 1207–1212. doi:10.1134/

S0031918X21120115.

[35] S. V. Dmitriev, E. A. Korznikova, A. P. Chetverikov, Supersonic N-crowdions in a two-dimensional Morse crystal, Journal of Experimental and Theoretical Physics 126 (3) (2018) 347–352.

[36] I. A. Shepelev, E. A. Korznikova, D. V. Bachurin, A. S. Semenov, A. P. Chetverikov, S. V. Dmitriev, Supersonic crowdion clusters in 2D Morse lattice, Physics Letters A 384 (1) (2020) 126032.

[37] E. A. Korznikova, I. R. Sunagatova, A. M. Bayazitov, A. S. Semenov, S. V. Dmitirev, Effect of interatomic potentials on mass transfer by supersonic 2-crowdions, Letters on Materials 9 (4) (2019) 386–390.

[38] S. V. Dmitriev, N. N. Medvedev, A. P. Chetverikov, K. Zhou, M. G. Velarde, Highly enhanced transport by supersonic N-crowdions, Physica Status Solidi (RRL)–Rapid Research Letters 11 (12) (2017) 1700298.

[39] R. I. Babicheva, I. Evazzade, E. A. Korznikova, I. A. Shepelev, K. Zhou, S. V. Dmitriev, Low-energy channel for mass transfer in Pt crystal initiated by molecule impact, Computational Materials Science 163 (2019) 248–255.

[40] A. M. Bayazitov, S. V. Dmitriev, P. V. Zakharov, I. A. Shepelev, S. Y. Fomin, E. A. Korznikova, Features of mass transfer by N-crowdions in fcc Ni_3Al lattice, in: IOP Conference Series: Materials Science and Engineering, Vol. 672, IOP Publishing, 2019, p. 012033.

[41] M. Rieth, S. L. Dudarev, S. M. Gonzalez De Vicente, J. Aktaa, T. Ahlgren, S. Antusch, D. E. J. Armstrong, M. Balden, N. Baluc, M.-F. Barthe, W. W. Basuki, M. Battabyal, C. S. Becquart, D. Blagoeva, H. Boldyryeva, J. Brinkmann, M. Celino, L. Ciupinski, J. B. Correia, A. De Backer, C. Domain, E. Gaganidze, C. García-Rosales, J. Gibson, M. R. Gilbert, S. Giusepponi, B. Gludovatz, H. Greuner, K. Heinola, T. Höschen, A. Hoffmann, N. Holstein, F. Koch, W. Krauss, H. Li, S. Lindig, J. Linke, C. Linsmeier, P. López-Ruiz, H. Maier, J. Matejicek, T. P. Mishra, M. Muhammed, A. Muñoz, M. Muzyk, K. Nordlund, D. Nguyen-Manh, J. Opschoor, N. Ordás, T. Palacios, G. Pintsuk, R. Pippan, J. Reiser, J. Riesch, S. G. Roberts, L. Romaner, M. Rosiński, M. Sanchez, W. Schulmeyer, H. Traxler, A. Ureña, J. G. Van Der Laan, L. Veleva, S. Wahlberg, M. Walter, T. Weber, T. Weitkamp, S. Wurster, M. A. Yar, J. H. You, A. Zivelonghi, Recent progress in research on tungsten materials for nuclear fusion applications in europe, Journal of Nuclear Materials 432 (1-3) (2013) 482–500. doi:10.1016/j.jnucmat.2012.08.018.

[42] G. Pintsuk, A. Hasegawa, Tungsten as a plasma-facing material, Comprehensive Nuclear Materials: Second Edition 6 (2020) 19–53.

[43] R. G. Abernethy, Predicting the performance of tungsten in a fusion environment: a literature review, Materials Science and Technology (United Kingdom) 33 (4) (2017) 388–399. doi:10.1080/02670836.2016.1185260.

[44] T. Muroga, J. Chen, V. Chernov, R. Kurtz, M. Le Flem, Present status of vanadium alloys for fusion applications, Journal of Nuclear Materials 455 (1-3) (2014) 263–268.

[45] D. Smith, J. Konys, T. Muroga, V. Evitkhin, Development of coatings for fusion power applications, Journal of Nuclear Materials 307-311 (2 SUPPL.) (2002) 1314–1322.

[46] D. R. Mason, D. Nguyen-Manh, M.-C. Marinica, R. Alexander, A. E. Sand, S. L. Dudarev, Relaxation volumes of microscopic and mesoscopic irradiation-induced defects in tungsten, Journal of Applied Physics 126 (7) (2019). doi:10.1063/1.5094852.

[47] A. Fellman, A. Sand, J. Byggmästar, K. Nordlund, Radiation damage in tungsten from cascade overlap with voids and vacancy clusters, Journal of Physics Condensed Matter 31 (40) (2019). doi:10.1088/1361-648X/ab2ea4.

[48] O. V. Ogorodnikova, L. Y. Dubov, S. V. Stepanov, D. Terentyev, Y. V. Funtikov, Y. V. Shtotsky, V. S. Stolbunov, V. Efimov, K. Gutorov, Annealing of radiation-induced defects in tungsten: Positron annihilation spectroscopy study, Journal of Nuclear Materials 517 (2019) 148–151. doi:10.1016/j.jnucmat.2019.02.010.

[49] L. Chen, L. Q. Li, H. R. Gong, J. L. Fan, W. Li, Irradiation effect on mechanical properties of tungsten from molecular dynamic simulation, Materials Letters 241 (2019) 27–30. doi:10.1016/j.matlet.2019.01.043.

[50] T. Koyanagi, N. A. P. Kiran Kumar, T. Hwang, L. M. Garrison, X. Hu, L. L. Snead, Y. Katoh, Microstructural evolution of pure tungsten neutron irradiated with a mixed energy spectrum, Journal of Nuclear Materials 490 (2017) 66–74. doi:10.1016/j.jnucmat.2017.04.010.

[51] C. Björkas, K. Nordlund, S. Dudarev, Modelling radiation effects using the ab-initio based tungsten and vanadium potentials, Nuclear Instruments and Methods in Physics Research Section B: Beam Interactions with Materials and Atoms 267 (18) (2009) 3204–3208.

[52] S. Han, L. A. Zepeda-Ruiz, G. J. Ackland, R. Car, D. J. Srolovitz, Interatomic potential for vanadium suitable for radiation damage simulations, Journal of Applied Pysics 93 (6) (2003) 3328–3335.

[53] W. Luo, R. Ahuja, Y. Ding, H.-K. Mao, Unusual lattice dynamics of vanadium under high pressure, Proceedings of the National Academy of Sciences of the United States of America 104 (42) (2007) 16428–16431. doi:10.1073/pnas.0707377104.

[54] S. P. Fitzgerald, Structure and dynamics of crowdion defects in bcc metals, Journal of Micromechanics and Molecular Physics 3 (03n04) (2018) 1840003.

[55] R. I. Garber, A. I. Fedorenko, Focusing of atomic collisions in crystals, Phys. Usp. 7 (4) (1964) 479–507. doi:10.3367/UFNr.0083.196407a.0385.

[56] A. I. Dmitriev, A. Y. Nikonov, Features of the Σ5 and Σ9 grain boundaries migration in bcc and fcc metals under shear loading–a molecular dynamics study, Facta Universitatis, Series: Mechanical Engineering 15 (2) (2017) 285–294.

[57] K. Nordlund, Historical review of computer simulation of radiation effects in materials, Journal of Nuclear Materials 520 (2019) 273–295.

[58] Y. Hong, N. Zhang, L. Xiong, Nanoscale plastic deformation mechanisms of single crystalline silicon under compression, tension and indentation, Journal of Micromechanics and Molecular Physics 1 (03n04) (2016) 1640007.

[59] B. Liu, L. Bai, E. A. Korznikova, S. V. Dmitriev, A. W.-K. Law, K. Zhou, Thermal conductivity and tensile response of phosphorene nanosheets with vacancy defects, The Journal of Physical Chemistry C 121 (25) (2017) 13876–13887.

[60] L. Bai, N. Srikanth, E. A. Korznikova, J. A. Baimova, S. V. Dmitriev, K. Zhou, Wear and friction between smooth or rough diamond-like carbon films and diamond tips, Wear 372 (2017) 12–20.

[61] L. K. Rysaeva, E. A. Korznikova, R. T. Murzaev, D. U. Abdullina, A. A. Kudreyko, J. A. Baimova, D. S. Lisovenko, S. V. Dmitriev, Elastic damper based on the carbon nanotube bundle, Facta Universitatis, Series: Mechanical Engineering 18 (1) (2020) 001–012.

[62] S. V. Dmitriev, Discrete breathers in crystals: Energy localization and transport, Journal of Micromechanics and Molecular Physics 1 (02) (2016) 1630001.

[63] E. Barani, E. A. Korznikova, A. P. Chetverikov, K. Zhou, S. V. Dmitriev, Gap discrete breathers in strained boron nitride, Physics Letters A 381 (41) (2017) 3553–3557.

[64] Y. Kosevich, Charged ultradiscrete supersonic kinks and discrete breathers in nonlinear molecular chains with realistic interatomic potentials and electron-phonon interactions, in: Journal of Physics: Conference Series, Vol. 833, IOP Publishing, 2017, p. 012021.

[65] F. Granberg, J. Byggmästar, K. Nordlund, Defect accumulation and evolution during prolonged irradiation of fe and fecr alloys, Journal of Nuclear Materials 528 (2020) 151843.

[66] L. Malerba, Molecular dynamics simulation of displacement cascades in α-Fe: A critical review, Journal of Nuclear Materials 351 (1-3) (2006) 28–38.

[67] M.-C. Marinica, L. Ventelon, M. Gilbert, L. Proville, S. Dudarev, J. Marian, G. Bencteux, F. Willaime, Interatomic potentials for modelling radiation defects and dislocations in tungsten, Journal of Physics: Condensed Matter 25 (39) (2013) 395502.

[68] A. P. Chetverikov, I. A. Shepelev, E. A. Korznikova, A. A. Kistanov, S. V. Dmitriev, M. G. Velarde, Breathing subsonic crowdion in Morse lattices, Computational Condensed Matter 13 (2017) 59–64.

[69] A. D. B. Woods, S. H. Chen, Lattice dynamics of molybdenum, Solid State Communications 2 (8) (1964) 233–237. doi:10.1016/0038-1098(64)90370-9.

[70] M. Gilbert, S. Dudarev, Ab initio multi-string frenkel-kontorova model for a b = a/2[111] screw dislocation in bcc iron, Philosophical Magazine 90 (7-8) (2010) 1035–1061. doi:10.1080/14786430903049104.

[71] C. S. Becquart, A. De Backer, P. Olsson, C. Domain, Modelling the primary damage in Fe and W: Influence of the short range interactions on the cascade properties: Part 1 - energy transfer, Journal of Nuclear Materials 547 (2021) 152816. doi:https://doi.org/10.1016/j.jnucmat.2021.152816.

[72] P. Olsson, C. S. Becquart, C. Domain, Ab initio threshold displacement energies in iron, Materials Research Letters 4 (4) (2016) 219–225.

[73] D. Mason, D. Nguyen-Manh, C. Becquart, An empirical potential for simulating vacancy clusters in tungsten, Journal of Physics Condensed Matter 29 (50) (2017). doi:10.1088/1361-648X/aa9776.

[74] H. Heinisch, B. Singh, Stochastic annealing simulation of differential defect production in high energy cascades, Journal of Nuclear Materials 232 (2-3) (1996) 206–213. doi:10.1016/S0022-3115(96)00434-5.

[75] M. Caturla, Object kinetic monte carlo methods applied to modeling radiation effects in materials, Computational Materials Science 156 (2019) 452–459. doi:10.1016/j.commatsci.2018.05.024.

[76] N. Castin, G. Bonny, A. Bakaev, F. Bergner, C. Domain, J. Hyde, L. Messina, B. Radiguet, L. Malerba, The dominant mechanisms for the formation of solute-rich clusters in low-cu steels under irradiation, Materials Today Energy 17 (2020). doi:10.1016/j.mtener.2020.100472.

[77] J. Balbuena, L. Malerba, N. Castin, G. Bonny, M. Caturla, An object kinetic monte carlo method to model precipitation and segregation in alloys under irradiation, Journal of Nuclear Materials 557 (2021). doi:10.1016/j.jnucmat.2021.153236.

[78] A. M. Marjaneh, D. Saadatmand, I. Evazzade, R. I. Babicheva, E. G. Soboleva, N. Srikanth, K. Zhou, E. A. Korznikova, S. V. Dmitriev, Mass transfer in the Frenkel-Kontorova chain initiated by molecule impact, Physical Review E 98 (2) (2018) 023003.

[79] T. I. Mazilova, E. V. Sadanov, V. N. Voyevodin, V. A. Ksenofontov, I. M. Mikhailovskij, Impact-induced concerted mass transport on w surfaces by a voidion mechanism, Surface Science 669 (2018) 10–15.

[80] O. U. Uche, D. Perez, A. F. Voter, J. C. Hamilton, Rapid diffusion of magic-size islands by combined glide and vacancy mechanism, Physical Review Letters 103 (4) (2009) 046101.

[81] I. A. Shepelev, D. V. Bachurin, E. A. Korznikova, A. M. Bayazitov, S. V. Dmitriev, Mechanism of remote vacancy emergence by a supersonic crowdion cluster in a 2D Morse lattice, Chinese Journal of Physics 70 (2021) 355–362. doi:10.1016/j.cjph.2021.01.010.

[82] I. A. Shepelev, S. V. Dmitriev, A. A. Kudreyko, M. G. Velarde, E. A. Korznikova, Supersonic voidions in 2D Morse lattice, Chaos, Solitons and Fractals 140 (2020). doi:10.1016/j.chaos.2020.110217.

[83] I. A. Shepelev, D. V. Bachurin, E. A. Korznikova, S. V. Dmitriev, Energy exchange in m-crowdion clusters in 2D Morse lattice, European Physical Journal B 93 (9) (2020). doi:10.1140/epjb/e2020-10160-0.